Exploring the electronic and optical properties of AgInO2

K. C. Bhamu and K. R. Priolkar

Citation: AIP Conference Proceedings **1728**, 020429 (2016); doi: 10.1063/1.4946480
View online: http://dx.doi.org/10.1063/1.4946480
View Table of Contents: http://scitation.aip.org/content/aip/proceeding/aipcp/1728?ver=pdfcov
Published by the AIP Publishing

Exploring the Electronic and Optical Properties of $AgInO_2$

K.C. Bhamu[a] and K.R. Priolkar[b]

Department of Physics, Goa University, Taleigao Plateau-403260, Goa

[a]Corresponding author: kcbhamu85@gmail.com
[b]krpriolkar@gmail.com

Abstract: We computed the energy band and density of states for electronic properties while for optical properties we computed dielectric function, absorption coefficient, optical conductivity and refractive index. The origin of energy bands is interpreted in terms of density of states. The electronic transitions in energy bands are explained from frequency dependent dielectric constant. Our computed band structure predicts $AgInO_2$ as indirect band gap semiconductor while from optical properties we have predicted importance of $AgInO_2$ in photovoltaic applications. We also reported valence charge density for this compound. Our computed results are in better agreement with available experimental data than those of earlier theoretically reported.

INTRODUCTION

Since the discovery of delafossite transparent conducting oxides (TCOs), they are playing key role in opto-electronic devices such as solar cells, flat panel display and calculators. The discovery of p-type conductivity and transparency in $CuAlO_2$ thin films by Kawazoe et al. [1] established a new benchmark in transparent electronics with the development of basic building block of transparent electronics, pn-junction, using this wide band gap p-type semiconductor. Delafossite TCOs are electrical conductive materials with a comparably low absorption of light in visible spectrum of the solar radiation and frequently available for use in transparent electronics [2-8]. Otabe et al. [2] studied $AgInO_2$ (AIO) and they predicted n-type character of AIO thin films. This invention opened the door for the fabrication of pn-junction totally based on delafossite which is transparent for visible light and absorbs UV photons. Later, Shuntaro et al. [3] also studied the same compound but with pulse laser deposition technique and the results were followed that of reported by Otabe et al. [2]. The experimental studies [4-8] are dedicated to synthesis of AIO. There are very few studies [8, 10, 11] available for the explanation of electronic and optical properties of AIO. Sheets el al. [8] studied experimental and computational studies on AIO to understand the electronic and optical properties. They used Stuttgart TB-LMTO-ASA program for computation of electronic properties. Kumar and his group [10-11] explained electronic and optical properties of AIO by using Heyd–Scuseria–Ernzerhof (HSE06) functional which enables to use Perdew–Burke–Ernzerhof (PBE) as exchange-correlation and the Hartree–Fock (HF) exchange interaction. However, some disagreement exists on reported band gaps with optical band gaps which encouraged us to shed more light on electronic and optical properties with improved band gap.

CRYSTAL STRUCTURE AND COMPUTATIONAL DETAILS

The crystal structure of AIO has layered structure composed of layer stacking of Ag plane and O-In-O dumbbell like structure along the c-axis. This layer stacking of InO_2 determines the phase formation of AIO either in 3R (rhombohedral, #166 space group) or in 2H (hexagonal, #194 space group) structure. Owing to the fact that the energy difference between formation energy is very small for both the protypes [9, 10] and hence properties of this material not change much. We focus on 2H structure throughout this letter. To calculate electronic and optical properties of AIO, full potential augmented plan wave (FP-LAPW) scheme is used. Details of FP-LAPW can be found in [12-14]. In this scheme ground state density for the crystals is obtained by using the solution of Kohn-Sham

International Conference on Condensed Matter and Applied Physics (ICC 2015)
AIP Conf. Proc. 1728, 020429-1–020429-4; doi: 10.1063/1.4946480
Published by AIP Publishing. 978-0-7354-1375-7/$30.00

equations. The unit cell is divided into interstitial region and non-overlapping atomic spheres, known as Muffin-tin (MT) spheres, which are centered at the atomic sites. Within the MT spheres, the crystal potential is formed by spherical harmonics; while in the interstitial region is represented by plane waves. The radius of MT spheres (RMT) in AIO was set to 2.08, 2.20 and 1.79 a.u. for Ag, In and O, respectively. In order to achieve the convergence criteria, the following parameters were used: $R_{mt}K_{max}$ = 7, G_{max}=12 and l_{max}=10 where, R_{mt}, K_{max}, G_{max} and l_{max} are the smallest atomic radius in the unit cell, magnitude of the largest k vector in the plane wave expansion,cut off for the charge density andmaximum radial expansion, respectively.

RESULTS AND DISCUSSION

Electronic Properties

We have computed energy bands and density of stated for AIO using local density approximation (LDA), generalized gradient approximation (GGA) and modified Becke–Johnson (mBJ) potential. Except some fine structure the overall trends in band gaps computed using LDA, GGA and mBJ schemes are similar. The band gap computed using mBJ potential shows reasonable band gap and so we report here only mBJ based calculation. However the LDA, GGA based band gaps are also mentioned in Table 1. Fig. 1 shows the energy bands along high symmetric directions and in Fig. 2, we have shown density of states (DOS).

Table 1. Direct and indirect band gaps for AIO. The unit of band gap is eV.

Our results						Available results		
LDA		GGA		mBJ		Theoretical band gaps		Experimental band gap
E^{dir}	E^{ind}	E^{dir}	E^{ind}	E^{dir}	E^{ind}	E^{dir}	E^{ind}	E^{dir}
0.97	0.25	1	0.26	3.5	1.75	1.62[a] 0.6[b]	2.58[a]	4.1(2)[c]

[a]Ref. [10], [b]Rf. [8], [c]Ref. [2,3]

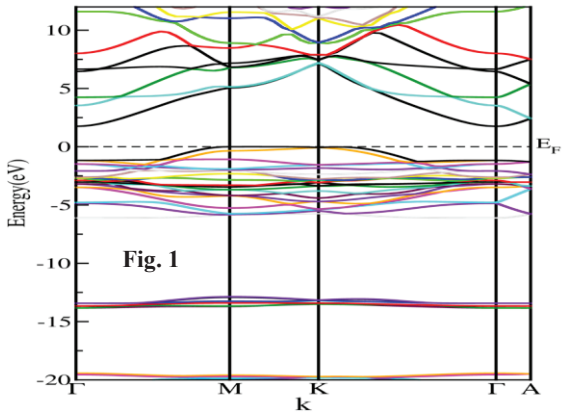

Fig. 1

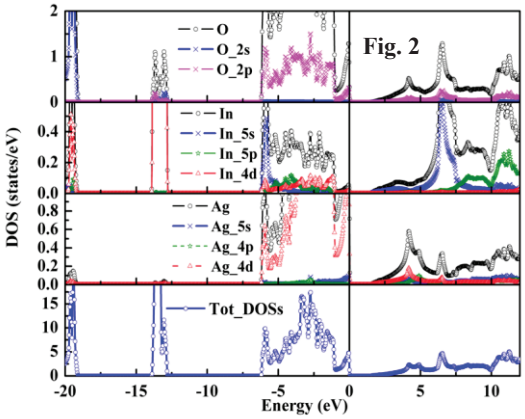

Fig. 2

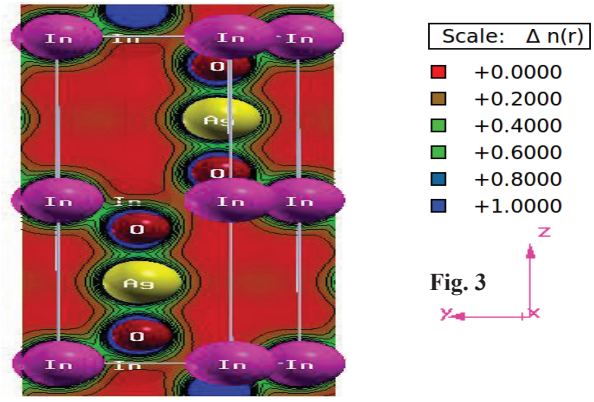

Fig. 3

Fig. 1: Band structure of $AgInO_2$.

Fig. 2: Density of statesof $AgInO_2$.

Fig. 3: Valence charge density for $AgInO_2$.

The empty region between VB and conduction region is band gap of AIO. We see from Fig. 1 that VB maximum is on M point while CB minimum is at r point which predicts the indirect band gap nature of AIO. The computed direct (indirect) band gap is found 3.5 (1.75.) eV which is in close agreement than experimental band gap 4.1(2) [2, 3] and is better than those band gaps reported by [5, 10, 11]. It is well known that energy bands can be explained in terms of DOS. For the same we have divide energy bands mainly in four groups: (a) bands in the bottom of the valence band (VB) region (b) bands in the middle of VB region (c) bands just below the Fermi level (dotted horizontal line) and (d) bands in the conduction region. The group (a) is originated by In-4d and O-2p states (Fig. 2). The group (b) is originated due to In-4d state with small contribution from O-2(s, p) states. The bands in group (c) are mainly due to strong hybridization between Ag-3d and O-2p states with negligible contribution from In-(5s, 4p) states. We see from Fig. 2 that just above the Fermi energy level there is no DOS and the same is retraced in energy bands where we see empty space. The absence of DOS in CB region is responsible for the band gap. Bands in the group (d) arises due to mixing of O-2p and In-5s in lower side while In-4p state is responsible for bands in higher CB region with small contribution from O-2p and Ag-4s. To shed more light on this explanation of energy bands in terms of DOS we have shown valence charge density in Fig. 3 along with Cartesian coordinate system and scale for charge density. From Fig. 3 we see that there is no charge distribution in red color region while along O-In and O-Ag bond it is between 0.4 to 0.6 e/a.u. This bonding plays the important roles in electronic properties. Charge density near O atom is highest which shows the influence of O atom is more than Ag and In which also can be seen from DOS where maximum contribution comes from O-2(s-p) states. This figure shows that charge distribution between Ag and In atoms is least.

Optical properties

Fig. 4 represents the imaginary (absorptive) part of frequency dependent dielectric function. Solid line and dotted lines represents the perpendicular and parallel components of dielectric function to the c-axis, respectively. Peaks in dielectric function arise due to direct interband transitions between VB and CB states. The amplitude of the dielectric function shows the interaction of electronic potential of the system to the incident photons. This interaction results in the electronic excitations causing interband transitions and these electronic transitions are responsible for peaks in the dielectric function. We see that below fundamental absorption edges (below 3.5eV) of AIO the amplitude remains almost zero. It means there is negligible interaction between incident photons and electronic potential of the system and hence the system is almost transparent in this energy range. As the energy of incident photon increases electronic potential of the system (AIO) start to interact with these incident photons.

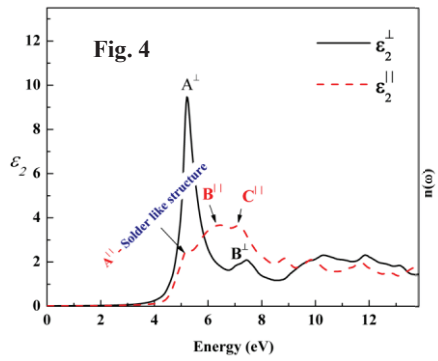

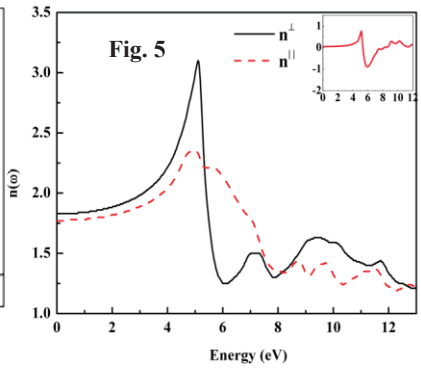

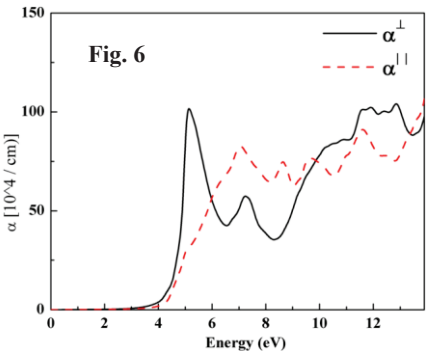

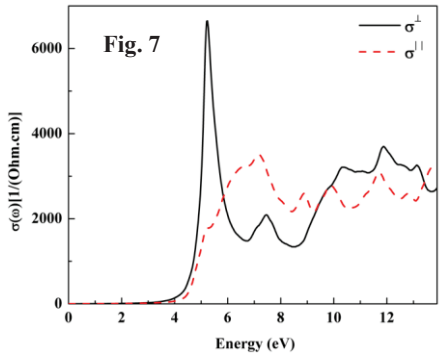

Fig. 4: Imaginary part of dielectric function.

Fig. 5: Refractive index of $AgInO_2$.

Fig. 6: Absorption coefficient for $AgInO_2$.

Fig. 7: Optical conductivity for $AgInO_2$

The first peaks in perpendicular components is located at 5.21eV which shows that at this energy our system greatly responds to incident photons and absorbs them. This energy range lies in the UV region of solar radiation. So we can say that AIO absorbs maximum incident photons in UV region. The later peaks in dielectric function also falls in UV region. The absorbance of photons in UV region makes AIO as a potential candidate photovoltaic technology like - AIO can be used as window layers of solar cells, in flat panel display, calculators and in solar watches. Fig. 5 represents the refractive index of AIO. We obtained the average value of RI 0.18 at zero frequency limit. The value of RI computed for LDA (GGA) is 0.23 (0.24). We see that the value of RI at zero frequency limit decreases in order to LDA, GGA and mBJ. Table 1 predicts that the value of band gaps increases from LDA to mBJ. This opposite trend in band gaps and RI is in accordance with the Penn model [15] and validates the accuracy of our calculations. In the inset of Fig. 5 have also plotted birefringence (difference between the perpendicular and parallel component). A linear curve in birefringence shows the isotropic while deviation from linearity shows the anisotropic behaviour of the system. In the present case we see that in AIO favours isotropic behaviour except at the energy around 5.0 to 6.0eV where it shows slight anisotropic behaviour.

The absorption coefficient and optical conductivity for AIO, computed using the mBJ potential are plotted in Fig. 6 and Fig. 7, respectively. From Fig. 6, it is seen that the absorption spectra starts above 3.5 eV and this value follows the fundamental band gap (3.5eV). We see the highest value of absorption coefficient and optical conductivity lies in the UV region and which envision the application of AIO in photovoltaic technology which is also confirmed but our dielectric function. The trends in our computed optical spectra are in agreement with [11].

CONCLUSIONS

We have computed energy bands and density of states for $AgInO_2$. Our computed band gap shows that $AgInO_2$ is an indirect band gap semiconductor. The computed indirect (direct) band gap is 1.75 eV (3.5) eV and in good agreement with experimentally reported band gap. Frequency dependent dielectric function envision the applications of $AgInO_2$ in transparent electronic. Our computed charge density contours predicts the role of oxygen atoms in unit cell of $AgIn_2$. Out results of refractive index, absorption coefficient and optical conductivity favours the conclusion drawn from dielectric function and hence depict the applicability of $AgInO_2$ in solar cells.

ACKNOWLEDGMENTS

Bhamu acknowledges UGC, New Delhi for his Kothari Fellowship [Letter No. 4-2/2006(BSR)/PH/13-14/0113].

REFERENCES

1. H. Kawazoe, M. Yasukawa, H. Hyodo, M. Kurita, H. Yanagi and H. Hosono, Nature **389**, 939-942 (1997).
2. T. Otabe, K. Ueda, A. Kudoh, H. Hosono and H. Kawazoe, Appl. Phys. Lett. **72**, 1036-1038 (1998).
3. S. Ibuki, H. Yanagi, K. Ueda, H. Kawazoe and H. Hosono, J. Appl. Phys. **88**, 3067-3069 (2000).
4. D. Y. Shahriari, N. Erdman, U. T. M. Haug, M. C. Zarzyczn, L. D. Marks, K. R. Poeppelmeier, J. Phys. Chem. Solids **64**, 1437–1441 (2003).
5. H. Dong, Z. Li, X. Xu, Z. Ding, L. Wu, X. Wang and X. Fu, Appl. Catal. B: Environ. **89**, 551-556 (2009).
6. R. Nagarajan, N. Duan, M. K. Jayaraj, J. Li, K. A. Vanaja, A. Yokochi, A. Draeseke, J. Tate and A. W. Sleight, Int. J. Inorg. Mater. **3**, 265-270 (2001).
7. S. Ouyang, N. Kikugawa, D. Chen, Z. Zou and J. Ye, J. Phys. Chem. C **113**, 1560-1566 (2009).
8. W. C. Sheets, E. S. Stampler, M. I. Bertoni, M. Sasaki, T. J. Marks, T. O. Mason and K. R. Poeppelmeier, Inorg. Chem. **47**, 2696-2705 (2008).
9. K. C. Bhamu, R. Khenata, S. A. Khan, M. Singh and K. R. Priolkar, J. Electron. Mater. **45**, 615-623 (2016).
10. M. Kumar, H. Zhao and C. Persson, Semicond. Sci. Technol. **28**, 065003-1-10 (2013).
11. M. Kumar and C. Persson, Physica B **422**, 20-27 (2013).
12. P. Blaha, K. Schwarz, G. Madsen, D. Kuasnicka, J. Luitz, (User's Guide, *WIEN2K_14.2*, Vienna University of Technology, Austria, 2014) pp.1-258.
13. K.C. Bhamu, A. Dashora, G. Arora and B. L. Ahuja, Radiat. Phys. Chem. **81**, 728-734 (2012).
14. K. C. Bhamu, J. Sahariya and B. L. Ahuja J. Phys. Chem. Solids **74**, 765-771 (2013).
15. P. R. Penn, Phys. Rev. **128**, 2093-2097 (1962).